

New transiting hot Jupiters discovered by WASP-South, Euler/CORALIE and TRAPPIST-South

Coel Hellier¹, D.R. Anderson¹, F. Bouchy², A. Burdanov³, A. Collier Cameron⁴, L. Delrez^{3,5}, M. Gillon³, E. Jehin³, M. Lendl⁶, L.D. Nielsen², P.F.L. Maxted¹, F. Pepe², D. Pollacco⁷, D. Queloz⁵, D. Ségransan², B. Smalley¹, A.H.M.J. Triaud⁸, S. Udry², and R.G. West⁷

¹ Astrophysics Group, Keele University, Staffordshire, ST5 5BG, UK

² Observatoire astronomique de l'Université de Genève 51 ch. des Maillettes, 1290 Sauverny, Switzerland

³ Space sciences, Technologies and Astrophysics Research (STAR) Institute, Université de Liège, Allée du 6 Août, 17, Bat. B5C, 4000 Liège, Belgium

⁴ SUPA, School of Physics and Astronomy, University of St. Andrews, North Haugh, Fife, KY16 9SS, UK

⁵ Cavendish Laboratory, J J Thomson Avenue, Cambridge, CB3 0HE, UK

⁶ Space Research Institute, Austrian Academy of Sciences, Schmiedlstr. 6, 8042, Graz, Austria

⁷ Department of Physics, University of Warwick, Gibbet Hill Road, Coventry CV4 7AL, UK

⁸ School of Physics & Astronomy, University of Birmingham, Edgbaston, Birmingham, B15 2TT, UK

date

ABSTRACT

We report the discovery of eight hot-Jupiter exoplanets from the WASP-South transit survey. WASP-144b has a mass of $0.44 M_{\text{Jup}}$, a radius of $0.85 R_{\text{Jup}}$, and is in a 2.27-d orbit around a $V = 12.9$, K2 star which shows a 21-d rotational modulation. WASP-145Ab is a $0.89 M_{\text{Jup}}$ planet in a 1.77-d orbit with a grazing transit. The host is a $V = 11.5$, K2 star with a companion 5 arcsecs away and 1.4 mags fainter. WASP-158b is a relatively massive planet at $2.8 M_{\text{Jup}}$ with a radius of $1.1 R_{\text{Jup}}$ and a 3.66-d orbit. It transits a $V = 12.1$, F6 star. WASP-159b is a bloated hot Jupiter ($1.4 R_{\text{Jup}}$ and $0.55 M_{\text{Jup}}$) in a 3.8-d orbit around a $V = 12.9$, F9 star. WASP-162b is a massive planet in a relatively long and highly eccentric orbit ($5.2 M_{\text{Jup}}$, $P = 9.6$ d, $e = 0.43$). It transits a $V = 12.2$, K0 star. WASP-168b is a bloated hot Jupiter ($0.42 M_{\text{Jup}}$, $1.5 R_{\text{Jup}}$) in a 4.15-d orbit with a grazing transit. The host is a $V = 12.1$, F9 star. WASP-172b is a bloated hot Jupiter ($0.5 M_{\text{Jup}}$; $1.6 R_{\text{Jup}}$) in a 5.48-d orbit around a $V = 11.0$, F1 star. WASP-173Ab is a massive planet ($3.7 M_{\text{Jup}}$) with a $1.2 R_{\text{Jup}}$ radius in a circular orbit with a period of 1.39 d. The host is a $V = 11.3$, G3 star, being the brighter component of the double-star system WDS23366–3437, with a companion 6 arcsecs away and 0.8 mags fainter. One of the two stars shows a rotational modulation of 7.9 d.

Key words: Planetary Systems – stars: individual (WASP-144, WASP-145A, WASP-158, WASP-159, WASP-162, WASP-168, WASP-172, WASP-173A)

1 INTRODUCTION

Hot-Jupiter exoplanets are relatively rare, being found in only $\sim 1\%$ of Solar-like stars. However, since they are the easiest planets to detect they are by far the commonest type of planet found by ground-based transit surveys such as WASP (Pollacco et al. 2006). Such planets produce relatively deep transits ($\sim 1\%$) that recur often owing to short orbital periods (1–10 d). A massive planet in a close-in orbit will also produce a radial-velocity signal large enough for verification with relatively small telescopes such as the Swiss Euler 1.2-m and its CORALIE spectrograph. The ease of studying hot Jupiters also makes them important targets for characterisation. As an example, the community *Early*

Release Science program for transiting exoplanets with the *James Webb Space Telescope* (Bean et al. 2018) has chosen WASP-18b, WASP-43b and WASP-79b as the prime targets.

The imminent *TESS* satellite (Ricker et al. 2016) will perform an all-sky transit survey that is expected to find any hot Jupiters transiting bright stars that the ground-based surveys have missed. In the meantime, several ground-based surveys are making ongoing discoveries including HAT-South (e.g. Henning et al. 2018), KELT (e.g. Johnson et al. 2018), MASCARA (e.g. Talens et al. 2017) and NGTS (e.g. Bayliss et al. 2017). Here we report the latest hot-Jupiter discoveries from the WASP-South transit survey, verified with the Euler/CORALIE spectrograph (e.g. Triaud et al. 2013) and with follow-up photometry from EulerCAM

Table 1. Observations

Facility	Date	Notes
WASP-144:		
WASP-South	2006 May–2012 Jun	29 500 points
CORALIE	2014 Jun–2016 Oct	16 RVs
TRAPPIST	2014 Aug 13	Blue-block
TRAPPIST	2014 Nov 17	Blue-block
TRAPPIST	2015 May 18	Blue-block
TRAPPIST	2014 Jun 12	Blue-block
EulerCAM	2015 Jun 28	NGTS filter
WASP-145:		
WASP-South	2008 Jun–2012 Jun	54 000 points
CORALIE	2014 Jun–2016 Aug	19 RVs
TRAPPIST	2014 Nov 09	z band
EulerCAM	2014 Nov 16	Gunn z filter
EulerCAM	2015 Jul 02	Gunn z filter
WASP-158:		
WASP-South	2008 Jun–2012 Nov	27 000 points
CORALIE	2014 Aug–2016 Oct	20 RVs
TRAPPIST	2016 Oct 12	$I + z$ band
EulerCAM	2016 Nov 03	NGTS filter
WASP-159:		
WASP-South	2006 Sep–2012 Feb	43 800 points
CORALIE	2014 Nov–2017 Mar	29 RVs
EulerCAM	2016 Dec 02	NGTS filter
WASP-162:		
WASP-South	2006 May–2012 Jun	37 400 points
CORALIE	2014 Apr–2017 May	18 RVs
TRAPPIST	2015 Jun 07	$I + z$ band
EulerCAM	2017 Jan 14	I_c filter
WASP-168:		
WASP-South	2006 Oct–2012 Mar	31 000 points
CORALIE	2014 Dec–2017 Apr	31 RVs
TRAPPIST	2016 Feb 05	$I + z$ band
TRAPPIST	2016 Sep 16	V band
EulerCAM	2016 Sep 16	I_c filter
WASP-172:		
WASP-South	2006 May–2012 Jun	35 000 points
CORALIE	2012 Apr–2017 Jun	38 RVs
TRAPPIST	2014 Feb 03	$I + z$ band
TRAPPIST	2014 Jun 20	$I + z$ band
EulerCAM	2015 Jul 03	Gunn r filter
TRAPPIST	2015 May 31	z' filter
WASP-173:		
WASP-South	2006 May–2011 Nov	19 000 points
CORALIE	2015 Sep–2016 Dec	18 RVs
EulerCAM	2016 Sep 21	Gunn z filter
TRAPPIST	2016 Oct 06	V filter
EulerCAM	2016 Oct 20	Gunn z filter

(e.g. Lendl et al. 2012) and from the robotic TRAPPIST-South photometer (e.g. Gillon et al. 2013).

2 OBSERVATIONS

WASP-South is an array of eight cameras that, for the observations reported here, each consisted of a 200-mm, f/1.8 Canon lenses with a 2k×2k CCD, giving a $7.8^\circ \times 7.8^\circ$ field. The cameras are all on the same mount, which rasters a set of fields with a typical 10-min cadence, recording stars in the range $V = 9\text{--}13$. Processed photometry is accumulated in a central archive where the multi-year dataset on each star is searched for transits (see Collier Cameron et al. 2007b).

After vetting of all candidates by eye, the best ones are sent for followup observations with TRAPPIST-South and Euler/CORALIE. The observations for each star are listed in Table 1. All of our methods are similar to those for previous WASP-South discovery papers (e.g. Hellier et al. 2014; Maxted et al. 2016; Hellier et al. 2017), and for this reason the presentation here is relatively concise.

3 SPECTRAL ANALYSIS

We report spectral analyses of the host stars made using the CORALIE spectra. Adopting methods as described by Doyle et al. (2013), we estimated the effective temperature, T_{eff} , from the H α line, and the surface gravity, $\log g$, from Na I D and Mg I b lines. We also report an indicative spectral type deduced from the T_{eff} estimates. We report [Fe/H] values determined from equivalent-width measurements of unblended Fe I lines. The errors that we quote for the abundances take into account the uncertainties in T_{eff} and $\log g$. The Fe I lines were also used to estimate the rotation speed, $v \sin i$, after convolving with the CORALIE instrumental resolution ($R = 55\,000$), and also combining with an estimate of the macroturbulence taken from Doyle et al. (2014). Lastly, we report lithium abundance values and corresponding age estimates using (Sestito & Randich 2005), though such estimates are unreliable. The parameters obtained from the analysis are given in the Tables for each system. Where available we also list parallax values from the GAIA DR1 (Gaia Collaboration et al. 2016) and proper motions from the UCAC5 catalogue (Zacharias et al. 2017).

4 STELLAR ROTATIONAL MODULATIONS

The WASP photometry can span months of a year with observations on each clear night, and so is sensitive to rotational modulations down to the millimag level. We thus routinely search the photometry of planet hosts using a sine-wave fitting algorithm. We also compute a false alarm probability by repeatedly shuffling the nightly datasets (see Maxted et al. 2011). For most of the planet hosts in this paper we find only upper limits, but for WASP-144 and WASP-173 we found significant modulations.

5 SYSTEM PARAMETERS

As we have routinely done for previous planet-discovery papers, we combine the photometric and radial-velocity data sets for each system into one Markov-chain Monte-Carlo (MCMC) analysis, using a code originally described by Collier Cameron et al. (2007a). Since the CORALIE spectrograph underwent an upgrade in 2014 November we allow for a radial-velocity offset between the datasets before and after the upgrade (for future reference the RV values are listed in Table A1, where the time of upgrade is marked by a short line). The treatment of limb darkening is crucial to fitting transit photometry, and here we have used the 4-parameter, non-linear law of Claret (2000), interpolating coefficients for the appropriate stellar temperature and metallicity of each star.

On early MCMC runs we allowed the eccentricity to

be a free parameter, and for one of our systems (WASP-162b) we found a highly significant eccentricity. Where, however, the outcome was compatible with a circular orbit, we then computed results with a circular orbit imposed (this gives the most likely set of parameters, as discussed by Anderson et al. (2012), essentially feeding in the prior expectation that most hot Jupiters have orbits that have been circularised by tidal forces).

The list of MCMC parameters for the circular-orbit case is T_c (the epoch of mid-transit), P (the orbital period), ΔF (the transit depth that would be observed in the absence of limb-darkening), T_{14} (duration from first to fourth contact), b (the impact parameter) and K_1 (the stellar reflex velocity). The fitted parameters and other values derived from them are listed in a table for each system, along with $1-\sigma$ errors (though where no eccentricity is found we quote $2-\sigma$ upper limits). Red noise in the photometry could mean that the uncertainties are larger than quoted. For an account of the effects of red noise in datasets similar to those reported here see the analysis of multiple different transit lightcurves of WASP-36b by Smith et al. (2012).

An additional constraint on the fitting, continuing our practice from other recent discovery papers, comes from stellar models. We first run an MCMC analysis to estimate the stellar density (which can be derived from the transit lightcurve independently of a stellar model). We then use the stellar density and the spectroscopic effective temperature and metallicity to estimate the most likely stellar mass using the BAGEMASS code described in Maxted et al. (2015), which is based on the GARSTEC stellar evolution code (Weiss & Schlattl 2008). We then use a resulting stellar-mass estimate and its error as a Gaussian-prior input to the final MCMC analysis.

The masses and ages of the stars derived from BAGEMASS are given in Table 2. The best-fit stellar evolution tracks and isochrones are shown in Fig. 1.

6 WASP-144

The discovery photometry and radial-velocity data for WASP-144 are shown in Figs. 2 & 3. We also show the bisector spans, which are a check for transit mimics. The system parameters are listed in Table 3. WASP-144 is a relatively faint, $V = 12.9$, K2 star with a metallicity of $[Fe/H] = +0.18 \pm 0.14$. Evolutionary tracks suggest that it could be 8 ± 4 Gy old (Table 2).

The WASP data show a possible rotational modulation at a period of 21 ± 1 d with an amplitude of 4–8 mmag (see Fig. 4). This is seen independently in data from the seasons 2006 (7 mmag amplitude; false-alarm probability $<0.1\%$), 2011 (4-mmag amplitude; FAP 6%) and 2012 (8-mmag amplitude, FAP $<0.1\%$). The rotational period and fitted radius ($0.81 \pm 0.04 R_\odot$) imply a surface rotational velocity of $1.96 \pm 0.13 \text{ km s}^{-1}$, which compares with an observed $v \sin i$ of $1.9 \pm 1.2 \text{ km s}^{-1}$. Thus this is likely to be an aligned system (with the stellar spin axis perpendicular to us).

The followup photometry consists of four TRAPPIST-South transits and one from EulerCAM. The latter was observed in poor conditions with variable seeing, leading to systematic features in the lightcurve that we do not think

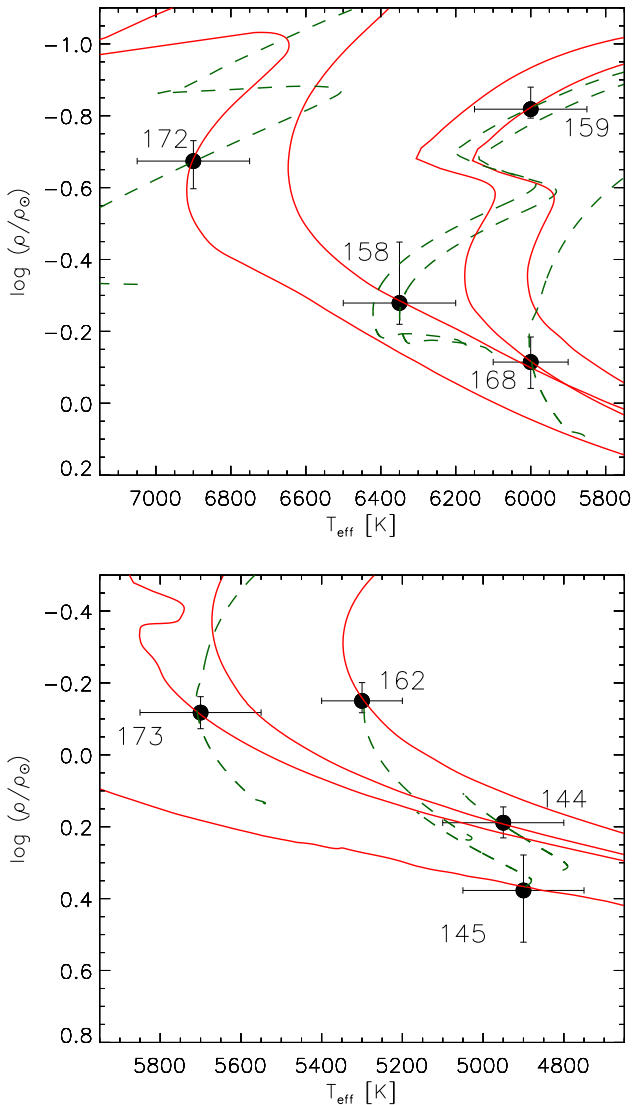


Figure 1. The host star's effective temperature (T_{eff}) versus density (each symbol being labelled by the WASP planet number). We show best-fit evolution tracks (dashed lines) and isochrones (solid lines) for the masses, ages and $[Fe/H]$ values listed in Table 2.

are astrophysically real. The MCMC process down-weighted this lightcurve in the fitting.

WASP-144b has a mass of $0.44 M_{\text{Jup}}$ and a radius of $0.85 R_{\text{Jup}}$ and is in a 2.27-d orbit. The radius of $0.85 R_{\text{Jup}}$ is among the lowest found for hot-Jupiter planets. Comparable planets are WASP-60b ($0.50 M_{\text{Jup}}$; $0.90 R_{\text{Jup}}$; Hébrard et al. 2013a) and Kepler-41b ($0.55 M_{\text{Jup}}$; $0.89 R_{\text{Jup}}$; Santerne et al. 2011). Both of those have G-star hosts whereas WASP-144 is a K2 star.

7 WASP-145

WASP-145A is a $V = 11.5$, K2 star, with solar metallicity ($[Fe/H] = +0.04 \pm 0.10$) and an estimated age of 7 ± 4 Gy (Figs. 5 & 6; Table 4).

Table 2. Mass and age estimates for the host stars, derived from the BAGEMASS code with GARSTEC stellar models and assuming $\alpha_{MLT} = 1.78$. Columns 2, 3 and 4 give the maximum-likelihood estimates of the age, mass, and initial metallicity, respectively. Column 5 is the chi-squared statistic of the fit for the parameter values in columns 2, 3, and 4. Columns 6 and 7 give the mean and standard deviation of their posterior distributions. The systematic errors on the mass and age due to uncertainties in the mixing length and helium abundance are given in columns 8 to 11.

Star	$\tau_{\text{iso},b}$ [Gyr]	$M_b[M_\odot]$	$[\text{Fe}/\text{H}]_{i,b}$	χ^2	$\langle \tau_{\text{iso}} \rangle$ [Gyr]	$\langle M_\star \rangle [M_\odot]$	$\sigma_{\tau,Y}$	$\sigma_{\tau,\alpha}$	$\sigma_{M,Y}$	$\sigma_{M,\alpha}$
WASP-144	9.5	0.84	+0.238	0.01	8.71 ± 4.12	0.844 ± 0.046	1.96	3.96	-0.040	-0.026
WASP-145	0.0	0.79	-0.048	0.07	6.99 ± 4.40	0.763 ± 0.040	0.12	0.02	-0.034	-0.006
WASP-158	1.5	1.32	+0.252	0.01	1.93 ± 0.93	1.339 ± 0.092	0.01	0.75	-0.035	-0.030
WASP-159	4.1	1.33	+0.227	0.03	3.40 ± 0.95	1.431 ± 0.118	-0.08	1.04	-0.036	-0.103
WASP-162	13.7	0.94	+0.381	0.00	12.97 ± 2.35	0.953 ± 0.041	0.84	3.10	-0.044	-0.034
WASP-168	3.9	1.08	+0.046	0.01	3.96 ± 1.77	1.073 ± 0.053	0.35	1.65	-0.043	-0.034
WASP-172	1.7	1.48	-0.102	0.04	1.79 ± 0.28	1.472 ± 0.067	0.00	0.03	-0.050	-0.006
WASP-173	6.6	1.03	+0.225	0.00	6.78 ± 2.93	1.035 ± 0.072	0.51	2.35	-0.044	-0.037

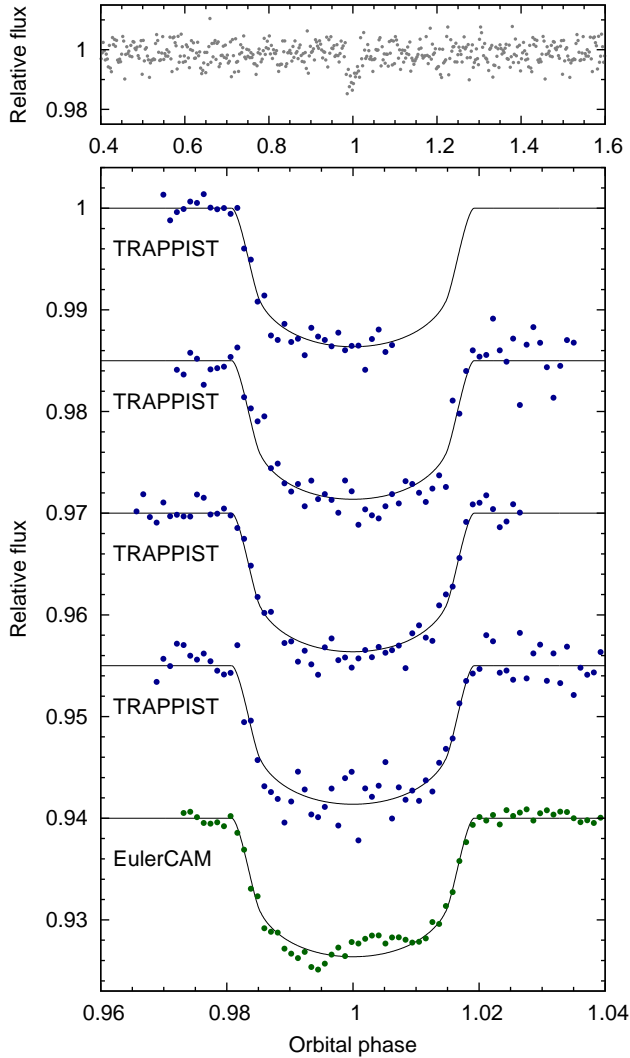


Figure 2. WASP-144b discovery photometry: (Top) The WASP data folded on the transit period. (Second panel) The binned WASP data with (offset) the follow-up transit lightcurves (ordered from the top as in Table 1) together with the fitted MCMC model.

Table 3. System parameters for WASP-144.

1SWASP J212303.08–400253.6
2MASS 21230309–4002537
GAIA RA = $21^{\text{h}}23^{\text{m}}03.09^{\text{s}}$, Dec = $-40^\circ 02' 54.4''$ (J2000)
V mag = 12.9
Rotational modulation: $P = 21 \pm 1$ d, 4–8 mmag
UCAC5 pm (RA) -3.4 ± 1.0 (Dec) -41.7 ± 1.0 mas/yr

Stellar parameters from spectroscopic analysis.

Spectral type	K2V
T_{eff} (K)	4950 ± 150
$\log g$	4.5 ± 0.2
$v \sin i$ (km s^{-1})	1.9 ± 1.2
[Fe/H]	$+0.18 \pm 0.14$
$\log A(\text{Li})$	< 0.6
Age (Lithium) [Gy]	> 0.5

Parameters from MCMC analysis.

P (d)	2.2783152 ± 0.0000013
T_c (HJD) (UTC)	$245\,7157.27493 \pm 0.00015$
T_{14} (d)	0.0814 ± 0.0007
$T_{12} = T_{34}$ (d)	0.0104 ± 0.0009
$\Delta F = R_p^2/R_*^2$	0.01165 ± 0.00028
b	0.45 ± 0.07
i ($^\circ$)	86.9 ± 0.5
K_1 (km s^{-1})	0.078 ± 0.011
γ (km s^{-1})	16.105 ± 0.008
e	0 (adopted) (< 0.30 at 2σ)
a/R_*	8.39 ± 0.23
M_* (M_\odot)	0.81 ± 0.04
R_* (R_\odot)	0.81 ± 0.04
$\log g_*$ (cgs)	4.53 ± 0.03
ρ_* (ρ_\odot)	1.54 ± 0.16
T_{eff} (K)	5200 ± 140
M_p (M_{Jup})	0.44 ± 0.06
R_p (R_{Jup})	0.85 ± 0.05
$\log g_p$ (cgs)	3.15 ± 0.06
ρ_p (ρ_J)	0.72 ± 0.15
a (AU)	0.0316 ± 0.0005
$T_{p,A=0}$ (K)	1260 ± 40

Errors are 1σ ; Limb-darkening coefficients were:
 r band: $a_1 = 0.734$ $a_2 = -0.714$, $a_3 = 1.399$, $a_4 = -0.614$

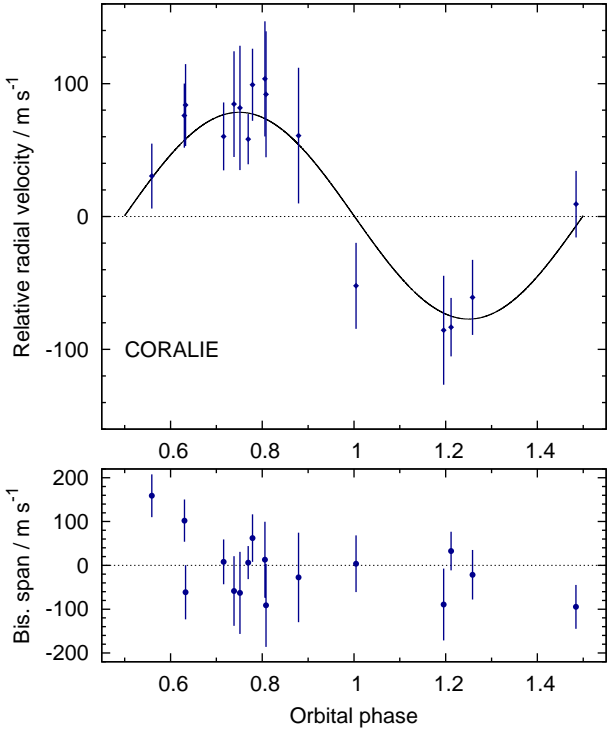


Figure 3. WASP-144b radial velocities and fitted model (top) along with (bottom) the bisector spans; the absence of any correlation with radial velocity is a check against transit mimics.

WASP-145A has a companion star, WASP-145B, separated by 5.14 ± 0.01 arcsecs with a position angle of -5.04 ± 0.13 degrees, and fainter by 1.407 ± 0.009 mag (as measured by focused EulerCAM images in a z' -band filter). It is likely that this star is physically associated with WASP-145A, but this is not certain. The later EulerCAM lightcurve (July 2015) was extracted using an aperture including both stars and this lightcurve was corrected for dilution in the analysis (the other follow-up lightcurves used a smaller aperture containing only the host star).

The planet WASP-145Ab has a 1.77-d orbit and a grazing transit ($b = 0.97 \pm 0.09$), which means that 2nd and 3rd contact are not discernable and thus that the planetary radius is not well constrained. We estimate the mass at $0.89 \pm 0.04 M_{Jup}$ and the radius at $0.9 \pm 0.4 R_{Jup}$. If the radius were at the lower end of that range it would be abnormally low for a hot Jupiter. The transit depth of 1.1% is typical for a hot Jupiter owing to a relatively small stellar radius of $0.68 \pm 0.07 R_\odot$.

8 WASP-158

WASP-158 is a $V = 12.1$, F6 star with a metallicity of $[Fe/H] = +0.24 \pm 0.15$. It is compatible with being an un-evolved main-sequence star with an age estimate of 1.9 ± 0.9 Gy.

The planet, WASP-158b, is relatively massive at $2.8 M_{Jup}$ with a radius of $1.1 R_{Jup}$, and has a 3.66-d orbit (Fig. 7; Table 5). WASP-158b is thus very similar to WASP-38b ($2.7 M_{Jup}$; $1.1 R_{Jup}$, in a 6.9-d orbit around an F8 star;

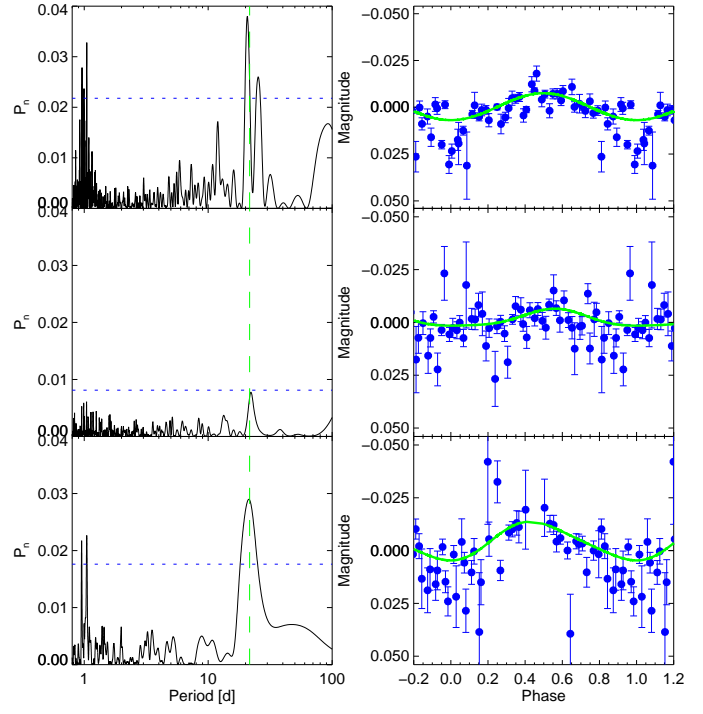


Figure 4. WASP-144 rotational modulation. The left-hand panels show periodograms for independent WASP-South data sets from 2006, 2011 and 2012. The blue dotted line is a false-alarm probability of 0.001. The right-hand panels show the data for each season folded on the 21-d period; the green line is a harmonic-series fit.

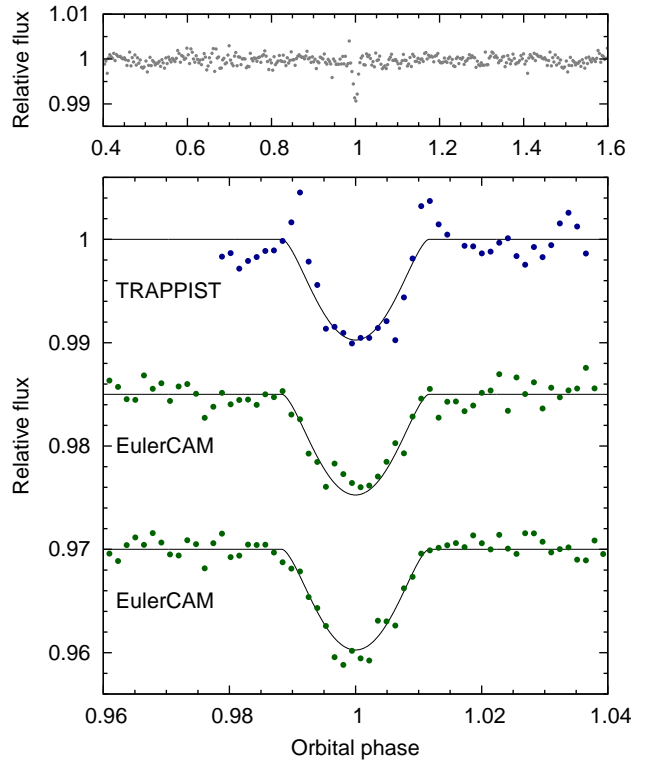


Figure 5. WASP-145b discovery photometry, as for Fig. 2.

Table 4. System parameters for WASP-145.

1SWASP J212900.65–585008.4
 2MASS 212900.65–585008.4
 GAIA RA = $21^{\text{h}}29^{\text{m}}00.90^{\text{s}}$, Dec = $-58^{\circ}50'10.1''$ (J2000)
 V mag = 11.5
 Rotational modulation < 2 mmag (95%)
 UCAC4 pm (RA) 102.6 ± 1.2 (Dec) 4.9 ± 3.4 mas/yr

Stellar parameters from spectroscopic analysis.	
Spectral type	K2V
T_{eff} (K)	4900 ± 150
$\log g$	4.6 ± 0.2
$v \sin i$ (km s^{-1})	2.1 ± 1.1
[Fe/H]	-0.04 ± 0.10
$\log A(\text{Li})$	< 0.5
Age (Lithium) [Gy]	> 0.5

Parameters from MCMC analysis.	
P (d)	1.7690381 ± 0.0000008
T_c (HJD) (UTC)	$245\,6844.16526 \pm 0.00026$
T_{14} (d)	0.0407 ± 0.0016
$T_{12} = T_{34}$ (d)	undefined
$\Delta F = R_p^2/R_*^2$	0.0116 ± 0.0026
b	0.97 ± 0.09
i ($^{\circ}$)	83.3 ± 1.3
K_1 (km s^{-1})	0.178 ± 0.006
γ (km s^{-1})	3.345 ± 0.005
e	0 (adopted) (< 0.06 at 2σ)
a/R_*	8.74 ± 0.52
M_* (M_{\odot})	0.76 ± 0.04
R_* (R_{\odot})	0.68 ± 0.07
$\log g_*$ (cgs)	4.65 ± 0.10
ρ_* (ρ_{\odot})	2.38 ± 0.93
T_{eff} (K)	4900 ± 150
M_p (M_{Jup})	0.89 ± 0.04
R_p (R_{Jup})	0.9 ± 0.4
$\log g_p$ (cgs)	3.4 ± 0.4
ρ_p (ρ_{J})	1.2 ± 1.0
a (AU)	0.0261 ± 0.0005
$T_{p,A=0}$ (K)	1200 ± 60

Errors are 1σ ; Limb-darkening coefficients were:

r band: $a1 = 0.703$, $a2 = -0.734$, $a3 = 1.472$, $a4 = -0.630$
 z band: $a1 = 0.765$, $a2 = -0.800$, $a3 = 1.258$, $a4 = -0.530$

Barros et al. 2011) and WASP-99b ($2.8 M_{\text{Jup}}$; $1.1 R_{\text{Jup}}$, in a 5.8-d orbit around an F8 star; Hellier et al. 2014).

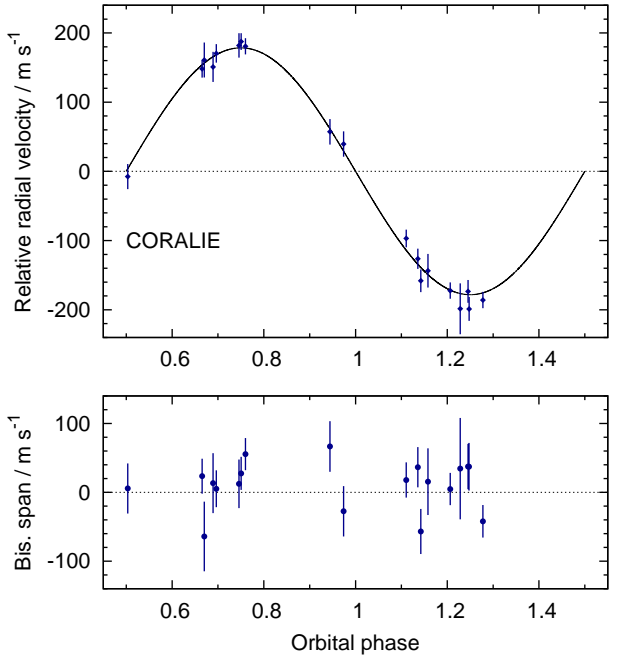
**Figure 6.** WASP-145b radial velocities and bisector spans, as for Fig. 3.

Table 5. System parameters for WASP-158.

1SWASP J001635.09–105834.9
 2MASS 001635.09–105834.9
 GAIA RA = $00^{\text{h}}16^{\text{m}}35.12^{\text{s}}$, Dec = $-10^{\circ}58'35.1''$ (J2000)
 V mag = 12.1
 Rotational modulation < 1.5 mmag (95%)
 UCAC5 pm (RA) 2.4 ± 1.2 (Dec) 0.4 ± 1.2 mas/yr
 GAIA DR1 parallax: 0.88 ± 0.57 mas

Stellar parameters from spectroscopic analysis.	
Spectral type	F6V
T_{eff} (K)	6350 ± 150
$\log g$	4.5 ± 0.2
$v \sin i$ (km s^{-1})	9.3 ± 1.3
[Fe/H]	$+0.24 \pm 0.10$
$\log A(\text{Li})$	< 1.7
Age (Lithium) [Gy]	(close to Lithium gap)

Parameters from MCMC analysis.	
P (d)	3.656333 ± 0.000004
T_c (HJD) (UTC)	$245\,7619.9195 \pm 0.0010$
T_{14} (d)	0.1490 ± 0.0037
$T_{12} = T_{34}$ (d)	0.014 ± 0.002
$\Delta F = R_p^2/R_*^2$	0.0063 ± 0.0005
b	0.32 ± 0.23
i ($^{\circ}$)	87.7 ± 1.5
K_1 (km s^{-1})	0.295 ± 0.015
γ (km s^{-1})	24.197 ± 0.012
e	0 (adopted) (< 0.16 at 2σ)
a/R_*	$8.0^{+0.4}_{-1.0}$
M_* (M_{\odot})	1.38 ± 0.14
R_* (R_{\odot})	1.39 ± 0.18
$\log g_*$ (cgs)	$4.30^{+0.05}_{-0.11}$
ρ_* (ρ_{\odot})	$0.53^{+0.08}_{-0.17}$
T_{eff} (K)	6350 ± 150
M_p (M_{Jup})	2.79 ± 0.23
R_p (R_{Jup})	1.07 ± 0.15
$\log g_p$ (cgs)	$3.75^{+0.06}_{-0.14}$
ρ_p (ρ_{J})	$2.3^{+0.5}_{-0.9}$
a (AU)	0.0517 ± 0.0018
$T_{p,A=0}$ (K)	1590 ± 80

Errors are 1σ ; Limb-darkening coefficients were:
 r band: $a_1 = 0.568$, $a_2 = 0.137$, $a_3 = 0.145$, $a_4 = -0.136$
 z band: $a_1 = 0.658$, $a_2 = -0.252$, $a_3 = 0.422$, $a_4 = -0.226$

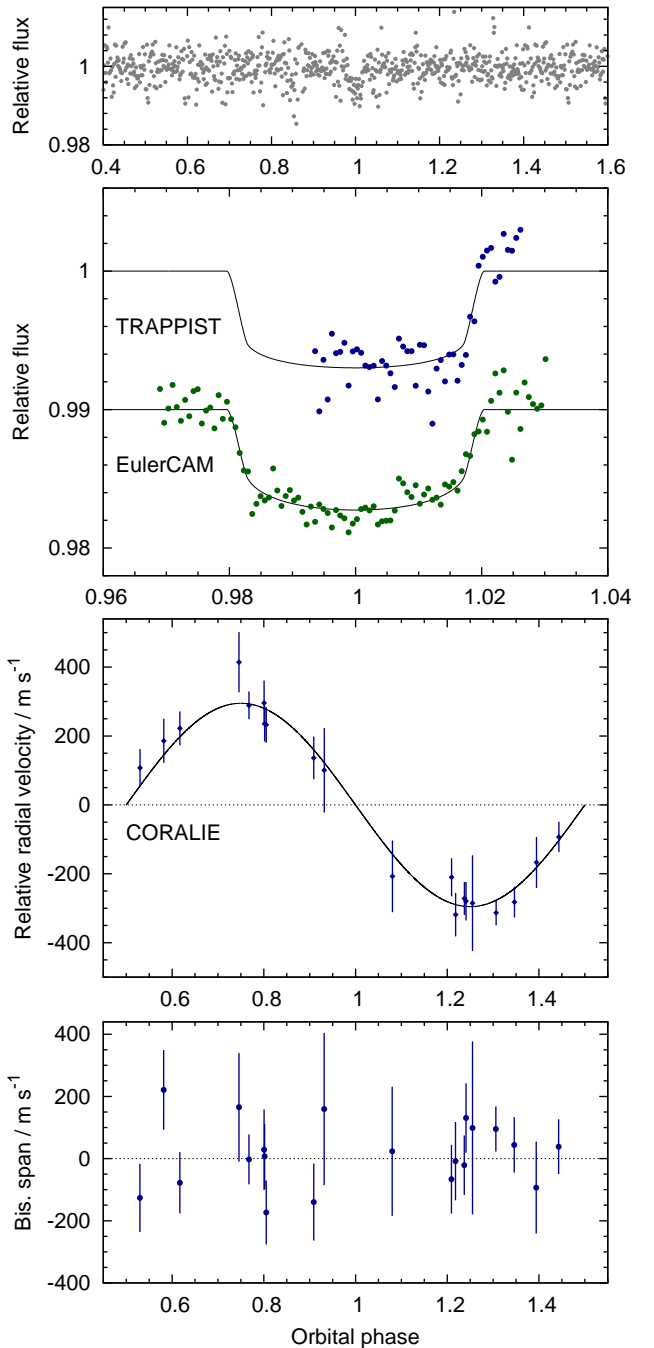
**Figure 7.** WASP-158b discovery data, as for Figs. 2 & 3.

Table 6. System parameters for WASP-159.

1SWASP J043232.73–385805.8
 2MASS 04323274–3858060
 GAIA RA = $04^{\text{h}}32^{\text{m}}32.76^{\text{s}}$, Dec = $-38^{\circ}58'06.0''$ (J2000)
 V mag = 12.8
 Rotational modulation < 1.5 mmag (95%)
 UCAC5 pm (RA) -0.9 ± 1.0 (Dec) 5.2 ± 1.0 mas/yr
 GAIA parallax: 1.08 ± 0.24 mas

Stellar parameters from spectroscopic analysis.	
Spectral type	F9
T_{eff} (K)	6000 ± 150
$\log g$	4.0 ± 0.1
$v \sin i$ (km s^{-1})	5.7 ± 0.4
[Fe/H]	$+0.22 \pm 0.12$
$\log A(\text{Li})$	2.15 ± 0.12
Age (Lithium) [Gy]	2 to 8
Parameters from MCMC analysis.	
P (d)	3.840401 ± 0.000007
T_c (HJD) (UTC)	$245\,7668.0849 \pm 0.0009$
T_{14} (d)	0.2328 ± 0.0021
$T_{12} = T_{34}$ (d)	0.0152 ± 0.0016
$\Delta F = R_P^2/R_*^2$	0.00453 ± 0.00018
b	0.18 ± 0.15
i ($^{\circ}$)	88.1 ± 1.4
K_1 (km s^{-1})	0.057 ± 0.008
γ (km s^{-1})	35.160 ± 0.006
e	0 (adopted) (< 0.18 at 2σ)
a/R_*	$5.44^{+0.15}_{-0.29}$
M_* (M_\odot)	1.41 ± 0.12
R_* (R_\odot)	2.11 ± 0.10
$\log g_*$ (cgs)	3.94 ± 0.04
ρ_* (ρ_\odot)	0.15 ± 0.02
T_{eff} (K)	6120 ± 140
M_P (M_{Jup})	0.55 ± 0.08
R_P (R_{Jup})	1.38 ± 0.09
$\log g_P$ (cgs)	2.82 ± 0.07
ρ_P (ρ_J)	0.21 ± 0.04
a (AU)	0.0538 ± 0.0015
$T_{\text{P},A=0}$ (K)	1850 ± 50
Errors are 1σ ; Limb-darkening coefficients were: r band: $a_1 = 0.595$, $a_2 = 0.011$, $a_3 = 0.345$, $a_4 = -0.220$	

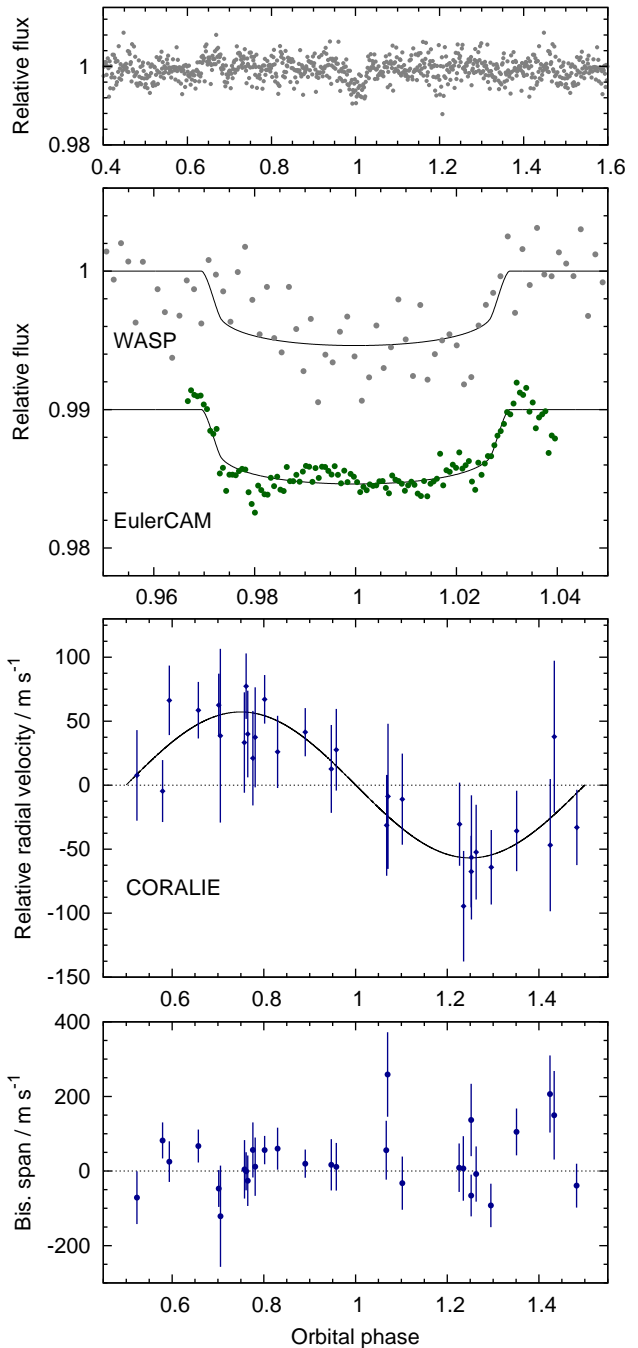
9 WASP-159

WASP-159 (Fig. 8; Table 6) is a fainter, $V = 12.9$, F9 star with a metallicity of $[\text{Fe}/\text{H}] = +0.22 \pm 0.12$. It appears to be evolving off the main sequence with a radius of 2.1 ± 0.1 R_\odot and an age estimate of 3.4 ± 1.0 Gy (Fig. 1; Table 2).

The fact that the stellar radius is expanded means that the transit depth is relatively small for a transiting hot Jupiter at 0.45%. This depth still equates to a fairly bloated planet ($1.4 \text{ R}_{\text{Jup}}$ and $0.55 \text{ M}_{\text{Jup}}$). This is a well-populated region of a hot-Jupiter mass–radius plot, no doubt in part because bloated planets are easiest to find in ground-based transit surveys.

10 WASP-162

WASP-162 is a $V = 12.2$, K0 star with a metallicity of $[\text{Fe}/\text{H}] = +0.28 \pm 0.13$. It appears to be old, with an expanded

**Figure 8.** WASP-159b discovery data as for Figs. 2 & 3.

radius for a low-mass star ($R = 1.11 \pm 0.05 \text{ R}_\odot$; $M = 0.95 \pm 0.05 \text{ M}_\odot$) leading to an age estimate of 13 ± 2 Gy. This star may have an inflated radius owing to magnetic activity. This phenomenon can be accounted for to some extent by using models with a lower mixing-length parameter (α_{MLT}). If we assume $\alpha_{\text{MLT}} = 1.50$ for this star instead of standard value of $\alpha_{\text{MLT}} = 1.78$ from a solar calibration, we obtain a best-fit age of 9.2 Gyr.

The planet is massive, at $5.2 \pm 0.2 \text{ M}_{\text{Jup}}$, and is in a relatively long and eccentric orbit ($P = 9.6$ d, $e = 0.43$;

Table 7. System parameters for WASP-162.

1SWASP J111310.29–173928.1
 2MASS 11131028–1739280
 GAIA RA = $11^{\text{h}}13^{\text{m}}10.30^{\text{s}}$, Dec = $-17^{\circ}39'28.0''$ (J2000)
 V mag = 12.2
 Rotational modulation < 1 mmag (95%)
 UCAC5 pm (RA) 6.2 ± 1.2 (Dec) -8.1 ± 1.2 mas/yr

Stellar parameters from spectroscopic analysis.	
Spectral type	K0
T_{eff} (K)	5300 ± 100
$\log g$	4.5 ± 0.1
$v \sin i$ (km s^{-1})	1.0 ± 0.8
[Fe/H]	$+0.28 \pm 0.13$
$\log A(\text{Li})$	< 0.7
Age (Lithium) [Gy]	> 1

Parameters from MCMC analysis.	
P (d)	9.62468 ± 0.00001
T_c (HJD) (UTC)	$245\,7701.3816 \pm 0.0006$
T_{14} (d)	0.1774 ± 0.0015
$T_{12} = T_{34}$ (d)	0.016 ± 0.001
$\Delta F = R_P^2/R_*^2$	0.0087 ± 0.0003
b	0.18 ± 0.14
i ($^{\circ}$)	89.3 ± 0.5
K_1 (km s^{-1})	0.507 ± 0.008
γ (km s^{-1})	16.824 ± 0.004
e	0.434 ± 0.005
ω (deg)	-1.9 ± 2.2
a/R_*	$17.0^{+0.4}_{-0.6}$
M_* (M_{\odot})	0.95 ± 0.04
R_* (R_{\odot})	1.11 ± 0.05
$\log g_*$ (cgs)	4.33 ± 0.03
ρ_* (ρ_{\odot})	0.71 ± 0.07
T_{eff} (K)	5300 ± 100
M_P (M_{Jup})	5.2 ± 0.2
R_P (R_{Jup})	1.00 ± 0.05
$\log g_P$ (cgs)	4.33 ± 0.03
ρ_P (ρ_J)	5.2 ± 0.6
a (AU)	0.0871 ± 0.0013
$T_{P,A=0}$ (K)	910 ± 20

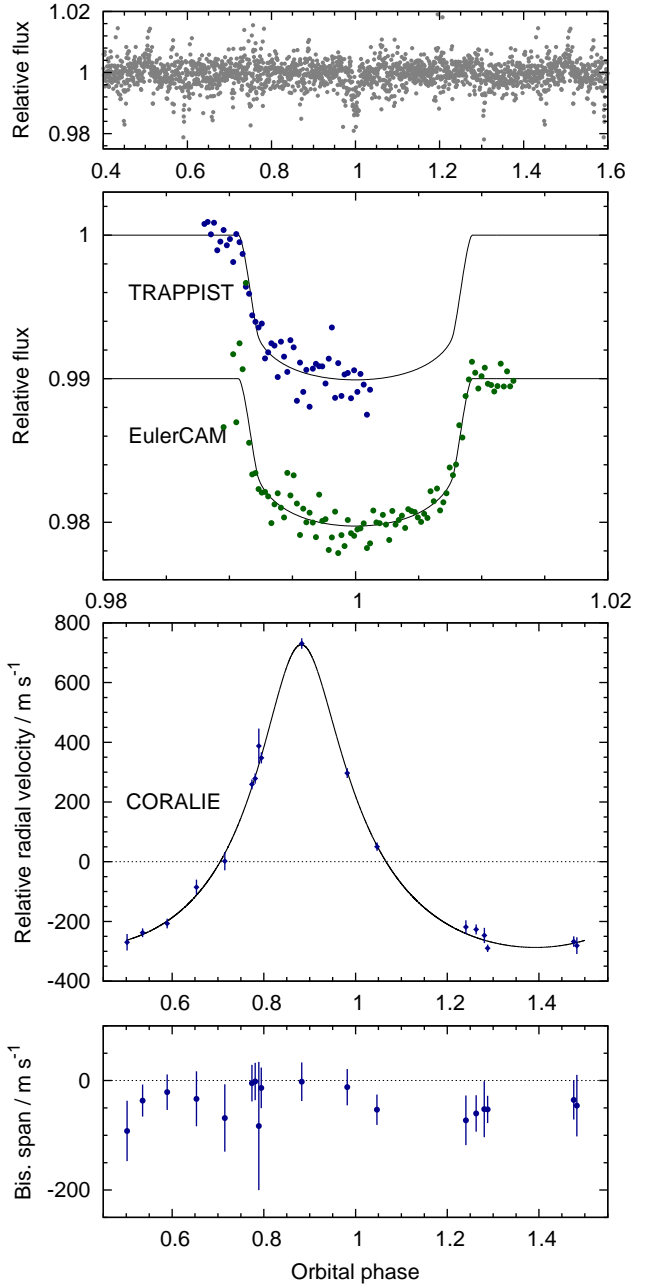
Errors are 1σ ; Limb-darkening coefficients were:
 r band: $a_1 = 0.750$, $a_2 = -0.724$, $a_3 = 1.393$, $a_4 = -0.614$
 z band: $a_1 = 0.826$, $a_2 = -0.863$, $a_3 = 1.266$, $a_4 = -0.540$
 I band: $a_1 = 0.827$, $a_2 = -0.881$, $a_3 = 1.376$, $a_4 = -0.598$

Fig. 9; Table 7). The circularisation timescale for such a planet (e.g. eqn 3 of Adams & Laughlin (2006), and assuming $Q_P \sim 10^5$) would be of order 30 Gyr, and so the eccentricity is compatible with the old age of the star. Given the transit, the probability that there is also an occultation of the planet (using eqn 2 of Kane & von Braun 2009) is greater than 0.46.

Comparable high-mass, long-period hot Jupiters in eccentric orbits include WASP-8b ($2.2 M_{\text{Jup}}$, 8.2 d, $e = 0.31$; Queloz et al. 2010) and Kepler-75 ($9.9 M_{\text{Jup}}$, 8.9 d, $e = 0.57$; Hébrard et al. 2013b).

11 WASP-168

WASP-168 (Figs. 10 & 11; Table 8) is a $V = 12.1$, F9 star with a metallicity of $[\text{Fe}/\text{H}] = -0.01 \pm 0.09$. The evolu-

**Figure 9.** WASP-162b discovery data, as for Figs. 2 & 3.

tional tracks indicate an age of 4 ± 2 Gy. The lithium abundance of $\log A(\text{Li}) 2.93 \pm 0.12$ indicates an age of < 1 Gy, though we consider this less reliable.

The planet has a 4.15-d orbit. Of the three follow-up transit lightcurves, note that the EulerCAM transit was observed simultaneously by TRAPPIST-South. These all show a grazing transit with a high impact factor ($b = 0.97 \pm 0.05$). As with WASP-145Ab, this means that the 2nd and 3rd contact are not discernable and thus that the planetary radius is not well constrained. Nevertheless, the estimates give a

Table 8. System parameters for WASP-168.

1SWASP 062658.70–464917.1
 2MASS 06265871–4649171
 GAIA RA = $06^{\text{h}}26^{\text{m}}58.71^{\text{s}}$, Dec = $-46^{\circ}49'17.2''$ (J2000)
 V mag = 12.1
 Rotational modulation < 3 mmag (95%)
 UCAC5 pm (RA) 0.0 ± 1.1 (Dec) 20.1 ± 1.1 mas/yr
 GAIA parallax: 3.13 ± 0.25 mas

Stellar parameters from spectroscopic analysis.	
Spectral type	F9V
T_{eff} (K)	6000 ± 100
$\log g$	4.0 ± 0.1
$v \sin i$ (km s^{-1})	0.3 ± 0.1
[Fe/H]	-0.01 ± 0.09
$\log A(\text{Li})$	2.93 ± 0.12
Age (Lithium) [Gy]	< 1

Parameters from MCMC analysis.	
P (d)	4.153658 ± 0.000003
T_c (HJD) (UTC)	$245\,7424.5278 \pm 0.0004$
T_{14} (d)	0.0797 ± 0.0017
$T_{12} = T_{34}$ (d)	undefined
$\Delta F = R_p^2/R_*^2$	$0.0119^{+0.0015}_{-0.0007}$
b	$0.97^{+0.06}_{-0.04}$
i ($^{\circ}$)	84.4 ± 0.6
K_1 (km s^{-1})	0.050 ± 0.004
γ (km s^{-1})	50.460 ± 0.003
e	0 (adopted) (< 0.09 at 2σ)
a/R_*	$9.59^{+0.65}_{-0.39}$
M_* (M_{\odot})	1.08 ± 0.05
R_* (R_{\odot})	1.12 ± 0.06
$\log g_*$ (cgs)	4.37 ± 0.05
ρ_* (ρ_{\odot})	0.77 ± 0.14
T_{eff} (K)	6000 ± 100
M_p (M_{Jup})	0.42 ± 0.04
R_p (R_{Jup})	$1.5^{+0.5}_{-0.3}$
$\log g_p$ (cgs)	2.6 ± 0.3
ρ_p (ρ_{J})	$0.12^{+0.10}_{-0.07}$
a (AU)	0.0519 ± 0.0008
$T_{\text{P},A=0}$ (K)	1340 ± 40

Errors are 1σ ; Limb-darkening coefficients were:
 r band: $a_1 = 0.547$, $a_2 = 0.084$, $a_3 = 0.308$, $a_4 = -0.215$
 z band: $a_1 = 0.633$, $a_2 = -0.263$, $a_3 = 0.523$, $a_4 = -0.280$
 V band: $a_1 = 0.462$, $a_2 = 0.310$, $a_3 = 0.181$, $a_4 = -0.170$
 I band: $a_1 = 0.627$, $a_2 = -0.208$, $a_3 = 0.518$, $a_4 = -0.286$

bloated planet with a mass of $0.42 \pm 0.04 M_{\text{Jup}}$ and a radius of $1.5^{+0.5}_{-0.3} R_{\text{Jup}}$. As noted for WASP-159b, bloated hot Jupiters with similar parameters are commonly found.

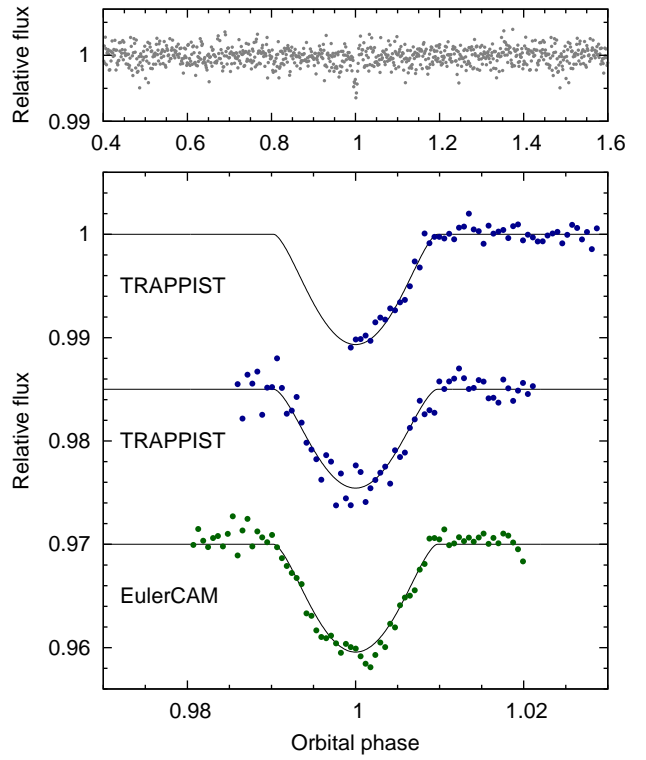
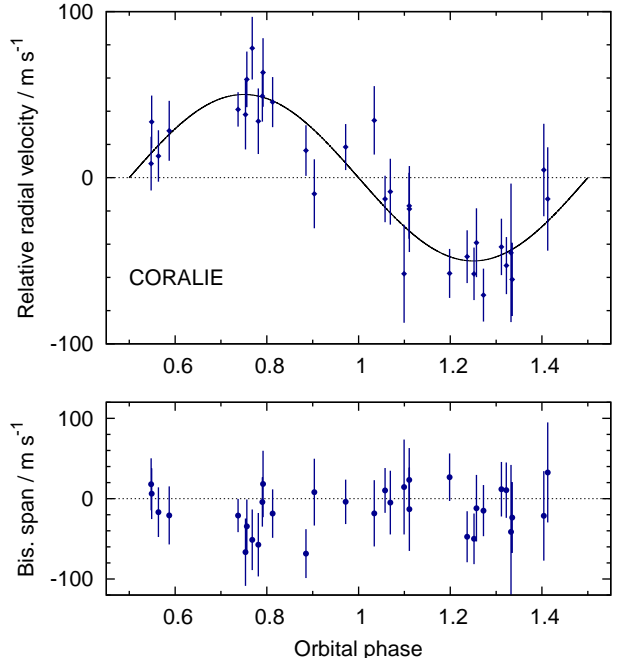
**Figure 10.** WASP-168b discovery photometry, as for Fig. 2.**Figure 11.** WASP-168b radial velocities and bisector spans, as for Fig. 3.

Table 9. System parameters for WASP-172.

1SWASP 131744.13–471415.3
 2MASS 13174412–4714152
 GAIA RA = $13^{\text{h}}17^{\text{m}}44.12^{\text{s}}$, Dec = $-47^{\circ}14'15.3''$ (J2000)
 V mag = 11.0
 Rotational modulation: < 1 mmag (95%)
 UCAC5 pm (RA) -16.2 ± 0.8 (Dec) 0.7 ± 0.8 mas/yr
 GAIA parallax: 1.78 ± 0.26 mas

Stellar parameters from spectroscopic analysis.	
Spectral type	F1V
T_{eff} (K)	6900 ± 150
$\log g$	4.1 ± 0.2
$v \sin i$ (km s^{-1})	13.7 ± 1.0
[Fe/H]	-0.10 ± 0.08
$\log A(\text{Li})$	< 1.2
Age (Lithium) [Gy]	(too hot for estimate)
Parameters from MCMC analysis.	
P (d)	5.477433 ± 0.000007
T_c (HJD) (UTC)	$245\,7032.2617 \pm 0.0005$
T_{14} (d)	0.2206 ± 0.0020
$T_{12} = T_{34}$ (d)	0.021 ± 0.002
$\Delta F = R_p^2/R_*^2$	0.0072 ± 0.0002
b	0.45 ± 0.12
i ($^{\circ}$)	86.7 ± 1.1
K_1 (km s^{-1})	0.042 ± 0.009
γ (km s^{-1})	-20.283 ± 0.006
e	0 (adopted) (< 0.28 at 2σ)
a/R_*	8.0 ± 0.5
M_* (M_{\odot})	1.49 ± 0.07
R_* (R_{\odot})	1.91 ± 0.10
$\log g_*$ (cgs)	4.05 ± 0.05
ρ_* (ρ_{\odot})	0.21 ± 0.04
T_{eff} (K)	6900 ± 140
M_p (M_{Jup})	0.47 ± 0.10
R_p (R_{Jup})	1.57 ± 0.10
$\log g_p$ (cgs)	2.64 ± 0.11
ρ_p (ρ_J)	0.12 ± 0.04
a (AU)	0.0694 ± 0.0011
$T_{\text{P},A=0}$ (K)	1740 ± 60

Errors are 1σ ; Limb-darkening coefficients were:
 r band: $a_1 = 0.422$, $a_2 = 0.603$, $a_3 = -0.477$, $a_4 = 0.129$
 z band: $a_1 = 0.513$, $a_2 = 0.159$, $a_3 = -0.089$, $a_4 = -0.018$

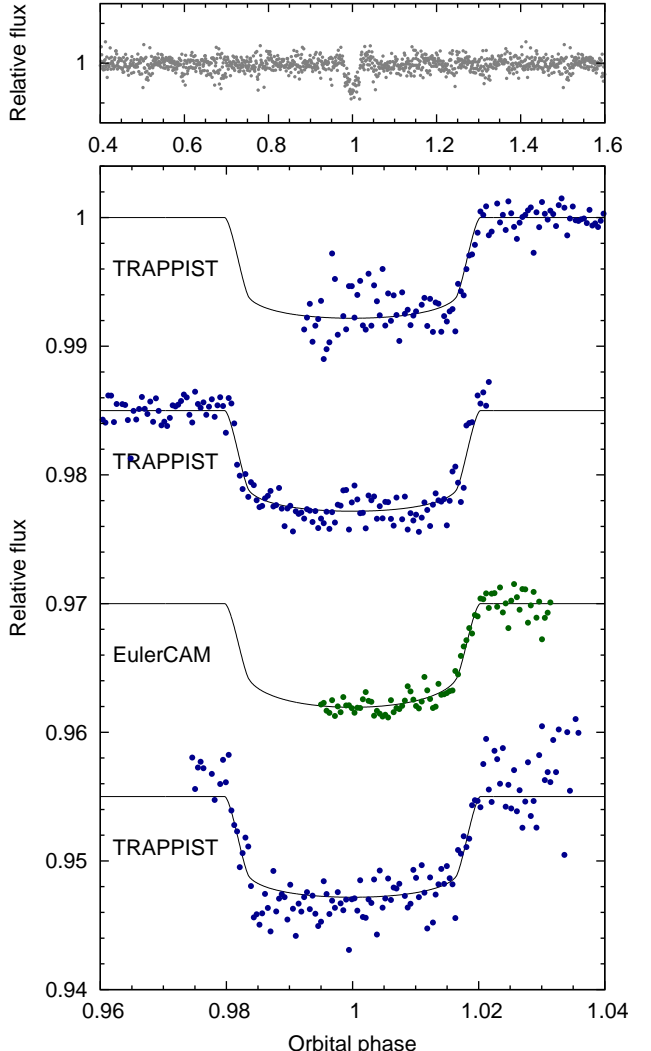
12 WASP-172

WASP-172 is a fairly hot, F1 star with $V = 11.0$ and a metallicity of $[\text{Fe}/\text{H}] = -0.10 \pm 0.08$. The age estimate is 1.8 ± 0.3 Gy. WASP-172b is a moderately bloated planet ($0.5 M_{\text{Jup}}$; $1.6 R_{\text{Jup}}$) in a 5.48-d orbit (Figs. 12 & 13; Table 9).

The large stellar radius ($1.9 R_{\odot}$) leads to a small transit depth of 0.7% and thus a ground-based survey would struggle to have detected the planet if it were not bloated. Thus, while highly irradiated hot Jupiters around hot stars are often found to be bloated one has to be careful with observational biases in constructing such samples.

13 WASP-173

WASP-173A (Figs. 14 & 15; Table 10) is the brighter component of a known double-star system catalogued as

**Figure 12.** WASP-172b discovery photometry, as for Fig. 2.

WDS23366–3437 (Mason et al. 2001). The two components have $V = 11.3$ and 12.1 and are separated by 6 arcsecs. Given the GAIA parallax of 4.34 ± 0.61 mas this amounts to a separation 1400 ± 200 AU. Our spectral analysis suggests a type of G3 and a metallicity of $+0.16 \pm 0.14$ for WASP-173A (we do not have spectra of the companion). The age estimate is 7 ± 3 Gy.

The WASP data show a rotational modulation at a period of 7.9 ± 0.1 d (Fig. 16). It is seen independently in three seasons (2006, 2007, 2011), with false-alarm probabilities of $< 0.1\%$ in two of them. The amplitude ranges from 6 to 15 mmag. Given the 14-arcsec pixels of WASP data we cannot tell which of the two stars is producing the modulation, but the amplitude suggests that it is more likely to be the brighter component, WASP-173A (note that the quoted amplitude has not been corrected for dilution). The follow-up transit lightcurves with EulerCAM and TRAPPIST-South used a smaller aperture containing only WASP-173A.

WASP-173Ab is a massive planet ($3.7 M_{\text{Jup}}$) in a close-in, circular orbit with a period of 1.39 d. The radius is $1.2 R_{\text{Jup}}$.

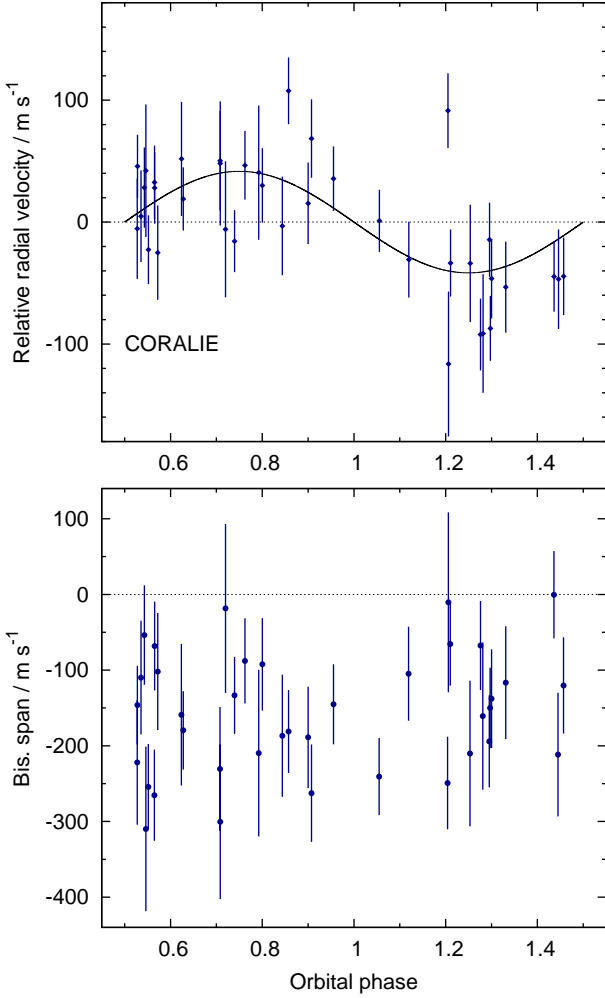


Figure 13. WASP-172b radial velocities and bisector spans, as for Fig. 3.

Given the stellar radius of $1.11 \pm 0.05 R_{\odot}$ the rotation period implies a surface velocity of $7.15 \pm 0.35 \text{ km s}^{-1}$. This compares with the measured $v \sin i$ of $6.1 \pm 0.3 \text{ km s}^{-1}$. This suggests that the spin axis might not be fully perpendicular to us, and thus that the planet might be in a moderately misaligned orbit. This system may be a worthwhile target for an observation of the Rossiter–McLaughlin effect.

14 DISCUSSION

To illustrate the newly discovered hot-Jupiter systems we plot some of their properties in Fig. 17. Blue symbols indicate the objects reported here; red symbols are from other recent WASP discovery papers (Temple et al. 2018; Lendl et al. 2018; Barkaoui et al. 2018; Demangeon et al. 2018; Anderson et al. 2018a, Anderson et al 2018c), while grey symbols are objects from the literature, including the recent HATSouth paper, Hartman et al. (2018).

The figure illustrates that the new systems lie within known parameter space, while being well distributed within the space. As is well established, the more massive planets

Table 10. System parameters for WASP-173.

1SWASP 233640.32–343640.4
2MASS 23364036–3436404
WDS23366–3437
GAIA RA = $23^{\text{h}}36^{\text{m}}40.38^{\text{s}}$, Dec = $-34^{\circ}36'40.6''$ (J2000)
V mag = 11.3
Rotational modulation: $P = 7.9 \pm 0.1$; 6–15 mmag amplitude
UCAC5 pm (RA) 88.1 ± 0.8 (Dec) -8.3 ± 0.8 mas/yr
GAIA parallax: 4.34 ± 0.61 mas
Stellar parameters from spectroscopic analysis.
Spectral type G3
T_{eff} (K) 5700 ± 150
$\log g$ 4.5 ± 0.2
$v \sin i$ (km s^{-1}) 6.1 ± 0.3
[Fe/H] $+0.16 \pm 0.14$
$\log A(\text{Li})$ < 0.8
Age (Lithium) [Gy] > 5
Parameters from MCMC analysis.
P (d) $1.38665318 \pm 0.00000027$
T_c (HJD) (UTC) $245\,7288.8585 \pm 0.0002$
T_{14} (d) 0.0957 ± 0.0007
$T_{12} = T_{34}$ (d) 0.0117 ± 0.0009
$\Delta F = R_P^2/R_*^2$ 0.0123 ± 0.0002
b 0.40 ± 0.08
i ($^{\circ}$) 85.2 ± 1.1
K_1 (km s^{-1}) 0.645 ± 0.007
γ (km s^{-1}) -7.858 ± 0.004
e 0 (adopted) (< 0.032 at 2σ)
a/R_* 4.78 ± 0.17
M_* (M_{\odot}) 1.05 ± 0.08
R_* (R_{\odot}) 1.11 ± 0.05
$\log g_*$ (cgs) 4.37 ± 0.03
ρ_* (ρ_{\odot}) 0.76 ± 0.08
T_{eff} (K) 5800 ± 140
M_P (M_{Jup}) 3.69 ± 0.18
R_P (R_{Jup}) 1.20 ± 0.06
$\log g_P$ (cgs) 3.77 ± 0.04
ρ_P (ρ_J) 2.14 ± 0.28
a (AU) 0.0248 ± 0.0006
$T_{P,A=0}$ (K) 1880 ± 55

Errors are 1σ ; Limb-darkening coefficients were:
 r band: $a1 = 0.673$, $a2 = -0.360$, $a3 = 0.893$, $a4 = -0.448$
 z band: $a1 = 0.754$, $a2 = -0.625$, $a3 = 0.957$, $a4 = -0.442$
 V band: $a1 = 0.602$, $a2 = -0.228$, $a3 = 0.902$, $a4 = -0.459$

are less likely to be highly bloated (top panel). The upper bound of planet radius in this plot is likely real while the lower bound could well involve selection effects, since smaller planets are harder to find in ground-based transit surveys, though whether this is the case will be established by the *TESS* survey. In common with past findings (e.g. Petigura et al. 2018) hot Jupiters are preferentially found around metal-rich stars (middle panel). The lower panel shows the marked decline in the hot Jupiter population at periods above 5–6 d (e.g. Hellier et al. 2017) which is too marked to be purely a selection effect caused by longer-period systems producing fewer transits and so being harder to find. The ongoing WASP survey is thus continuing to add to the statistics of the population, while finding some systems with exceptional properties (e.g. WASP-128b, Hodžić et al. 2018; WASP-189b, Anderson et al. 2018b),

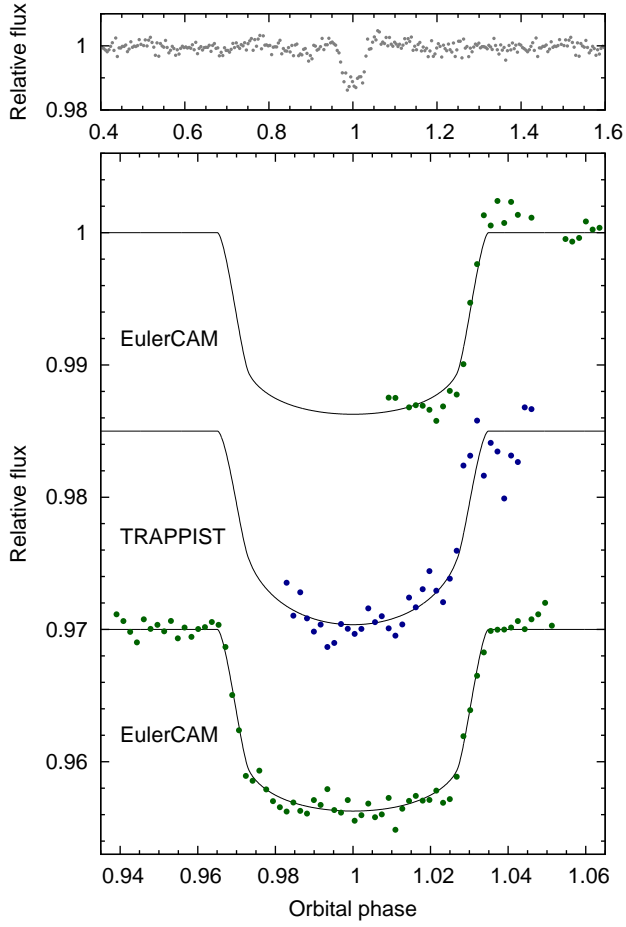


Figure 14. WASP-173b discovery photometry, as for Fig. 2.

and adding to the number of hot Jupiters transiting stars bright enough to allow atmospheric characterisation (e.g. Spake et al. 2018; Nikolov et al. 2018).

With regards to atmospheric characterisation the most promising of the new targets presented here is WASP-172b. This is a bloated, low-mass hot Jupiter ($0.47 M_{\text{Jup}}$; $1.57 R_{\text{Jup}}$) transiting a relatively bright star at $V = 11.0$. The atmosphere is also predicted to be hot (1740 ± 60 K) owing to the hot, F1 host star. Other bloated planets in this batch are WASP-159b, with a fainter host of $V = 12.9$, and WASP-168b, which has both a fainter host with $V = 12.1$ and a grazing transit making it harder to parametrise.

WASP-144b is notable for being un-bloated ($R = 0.85 \pm 0.05 R_{\text{Jup}}$). WASP-145b may also be unusually small for a hot Jupiter, but the radius has a large uncertainty owing to the transit being grazing.

Three of the planets reported here are relatively massive, WASP-158b at $2.8 M_{\text{Jup}}$, WASP-173Ab at $3.7 M_{\text{Jup}}$, and WASP-162b at $5.2 M_{\text{Jup}}$. Such planets are relatively less common. Before this paper, only 21 transiting hot Jupiters were known with masses in the range $2.5\text{--}6 M_{\text{Jup}}$ compared to 205 in the range $0.5\text{--}2.5 M_{\text{Jup}}$. Of the three new massive planets, only WASP-162b has a significant eccentricity ($e = 0.43$). Indeed WASP-173Ab is unusual in being a massive planet with no significant eccentricity (<0.032 at 2σ confidence), although this is likely explained its short orbital

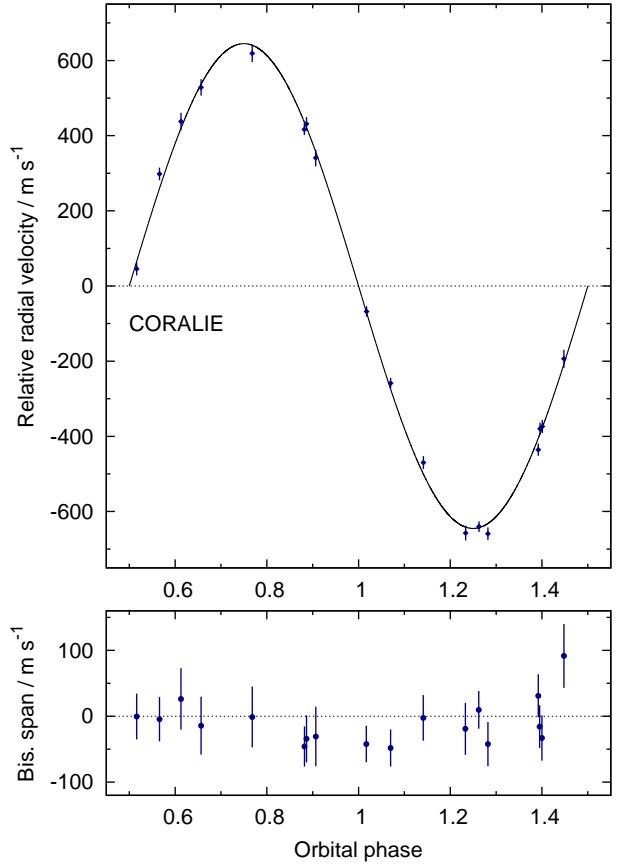


Figure 15. WASP-173b radial velocities and bisector spans, as for Fig. 3.

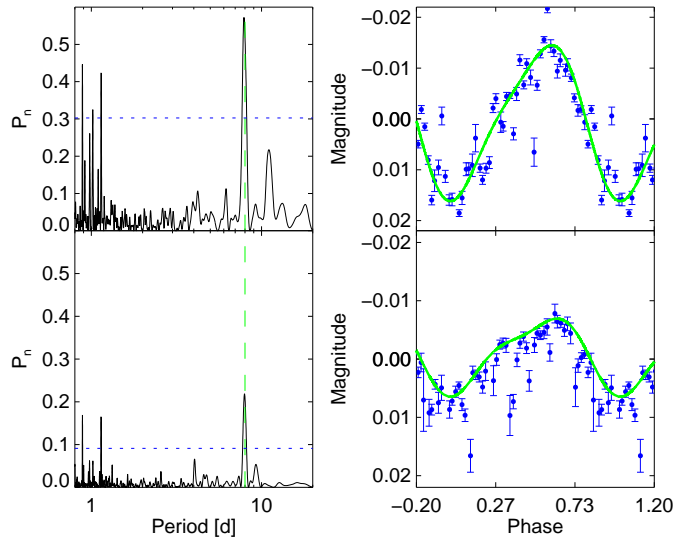


Figure 16. WASP-173 rotational modulation. The left-hand panels show periodograms for independent WASP data sets from 2007 and 2011. The blue dotted line is a false-alarm probability of 0.001. The right-hand panels show the data for each season folded on the 7.9-d period; the green line is a harmonic-series fit to the data

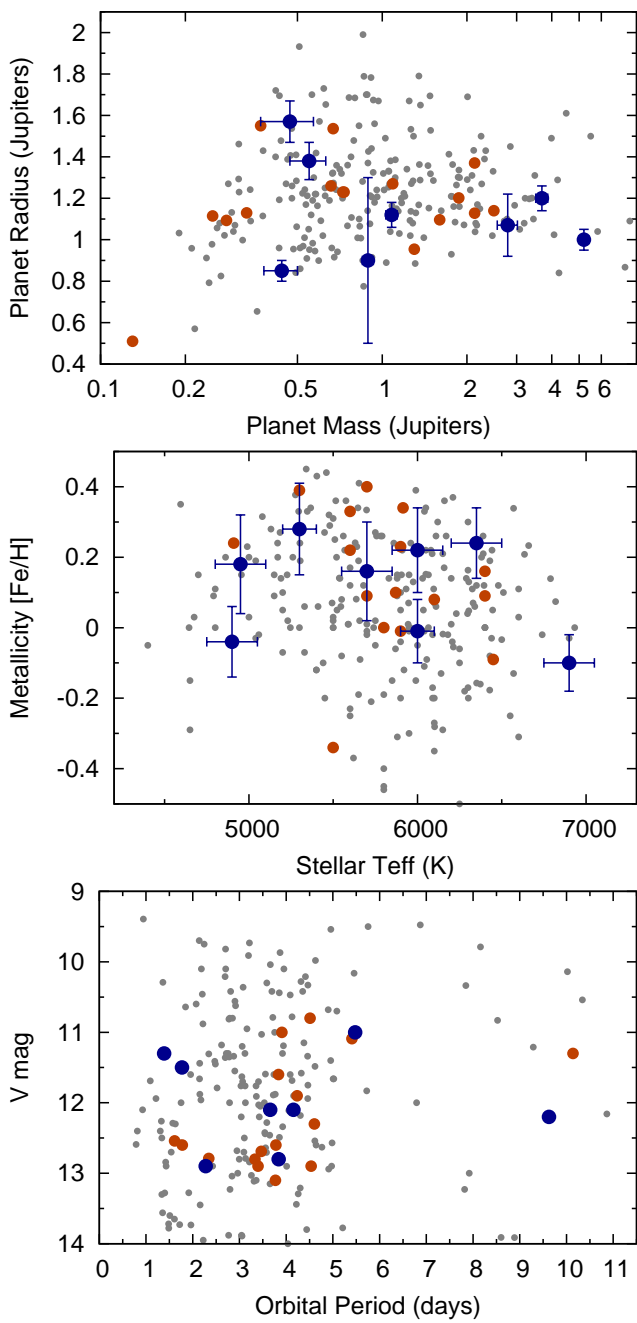


Figure 17. The new hot-Jupiter systems reported here (blue symbols) compared to recent WASP discoveries (red symbols) and previously known systems from the literature (grey). The figure shows planetary mass, radius and orbital period along with host-star temperature, metallicity and V -band magnitude.

period (1.39 d) leading to enhanced circularisation torques (e.g. Adams & Laughlin 2006).

Two of the planets reported here (WASP-145Ab and WASP-173Ab) are in double-star systems, adding to other recent WASP discoveries in binary systems (e.g. WASP-160Bb, (Lendl et al. 2018)). This is partly a result of WASP paying closer attention to candidates in binaries that were

ignored earlier in the project as being harder to observe. Overall, our results here show that the combination of WASP-South, CORALIE and TRAPPIST-South continues to be a productive team for discovering hot Jupiters transiting stars of $V < 13$.

ACKNOWLEDGEMENTS

WASP-South is hosted by the South African Astronomical Observatory and we are grateful for their ongoing support and assistance. Funding for WASP comes from consortium universities and from the UK's Science and Technology Facilities Council. The Euler Swiss telescope is supported by the Swiss National Science Foundation. TRAPPIST-South is funded by the Belgian Fund for Scientific Research (Fond National de la Recherche Scientifique, FNRS) under the grant FRFC 2.5.594.09.F, with the participation of the Swiss National Science Fund (SNF). The research leading to these results has received funding from the ARC grant for Concerted Research Actions, financed by the Wallonia-Brussels Federation. M.G. and E.J. are, respectively, Research Associate and Senior Research Associate at the FNRS-F.R.S. L.D. acknowledges support from a Gruber Foundation Fellowship.

REFERENCES

- Adams F. C., Laughlin G., 2006, *ApJ*, **649**, 1004
 Anderson D. R., et al., 2012, *MNRAS*, **422**, 1988
 Anderson D. R., et al., 2018a, preprint, ([arXiv:1809.07709](https://arxiv.org/abs/1809.07709))
 Anderson D. R., et al., 2018b, preprint, ([arXiv:1809.04897](https://arxiv.org/abs/1809.04897))
 Barkaoui K., et al., 2018, preprint, ([arXiv:1807.06548](https://arxiv.org/abs/1807.06548))
 Barros S. C. C., et al., 2011, *A&A*, **525**, A54
 Bayliss D., et al., 2017, preprint, ([arXiv:1710.11099](https://arxiv.org/abs/1710.11099))
 Bean J. L., et al., 2018, preprint, ([arXiv:1803.04985](https://arxiv.org/abs/1803.04985))
 Claret A., 2000, *A&A*, **363**, 1081
 Collier Cameron A., et al., 2007a, *MNRAS*, **375**, 951
 Collier Cameron A., et al., 2007b, *MNRAS*, **380**, 1230
 Demangeon O. D. S., et al., 2018, *A&A*, **610**, A63
 Doyle A. P., et al., 2013, *MNRAS*, **428**, 3164
 Doyle A. P., Davies G. R., Smalley B., Chaplin W. J., Elsworth Y., 2014, *MNRAS*, **444**, 3592
 Gaia Collaboration et al., 2016, *A&A*, **595**, A2
 Gillon M., et al., 2013, *A&A*, **552**, A82
 Hartman J. D., et al., 2018, preprint, ([arXiv:1809.01048](https://arxiv.org/abs/1809.01048))
 Hébrard G., et al., 2013a, *A&A*, **549**, A134
 Hébrard G., et al., 2013b, *A&A*, **554**, A114
 Hellier C., et al., 2014, *MNRAS*, **440**, 1982
 Hellier C., et al., 2017, *MNRAS*, **465**, 3693
 Henning T., et al., 2018, *AJ*, **155**, 79
 Hodžić V., et al., 2018, preprint, ([arXiv:1807.07557](https://arxiv.org/abs/1807.07557))
 Johnson M. C., et al., 2018, *AJ*, **155**, 100
 Kane S. R., von Braun K., 2009, *PASP*, **121**, 1096
 Lendl M., et al., 2012, *A&A*, **544**, A72
 Lendl M., et al., 2018, preprint, ([arXiv:1807.06973](https://arxiv.org/abs/1807.06973))
 Mason B. D., Wycoff G. L., Hartkopf W. I., Douglass G. G., Worley C. E., 2001, *AJ*, **122**, 3466
 Maxted P. F. L., et al., 2011, *PASP*, **123**, 547
 Maxted P. F. L., Serenelli A. M., Southworth J., 2015, *A&A*, **575**, A36
 Maxted P. F. L., et al., 2016, *A&A*, **591**, A55
 Nikolov N., et al., 2018, *Nature*, **557**, 526
 Petigura E. A., et al., 2018, *AJ*, **155**, 89
 Pollacco D. L., et al., 2006, *PASP*, **118**, 1407
 Queloz D., et al., 2010, *A&A*, **517**, L1
 Ricker G. R., et al., 2016, in Space Telescopes and Instrumentation 2016: Optical, Infrared, and Millimeter Wave. p. 99042B,
[doi:10.1117/12.2232071](https://doi.org/10.1117/12.2232071)
 Santerne A., Bonomo A. S., Hébrard G., Deleuil M., Moutou C., Almenara J.-M., Bouchy F., Díaz R. F., 2011, *A&A*, **536**, A70
 Sestito P., Randich S., 2005, *A&A*, **442**, 615
 Smith A. M. S., et al., 2012, *AJ*, **143**, 81
 Spake J. J., et al., 2018, *Nature*, **557**, 68
 Talens G. J. J., et al., 2017, *A&A*, **606**, A73
 Temple L. Y., et al., 2018, *MNRAS*, **480**, 5307
 Triaud A. H. M. J., et al., 2013, *A&A*, **551**, A80
 Weiss A., Schlattl H., 2008, *Ap&SS*, **316**, 99
 Zacharias N., Finch C., Frouard J., 2017, *AJ*, **153**, 166

Table A1. Radial velocities.

BJD – 2400 000 (UTC)	RV (km s ⁻¹)	σ_{RV} (km s ⁻¹)	Bisector (km s ⁻¹)
WASP-144:			
56837.74442	16.1865	0.0468	-0.0628
56845.73476	16.0438	0.0282	-0.0215
56926.63966	16.1629	0.0189	0.0062
56927.64776	16.0215	0.0220	0.0326
56928.60109	16.1807	0.0241	0.1021
56930.71731	16.1352	0.0244	0.1589
56931.73201	16.0526	0.0324	0.0036
56942.60950	16.2039	0.0271	0.0623
56955.60807	16.1140	0.0251	-0.0947
56958.62456	16.1967	0.0474	-0.0913
56983.52692	16.1859	0.0398	-0.0585
57140.88455	16.2049	0.0434	0.0129
57325.59467	16.1622	0.0510	-0.0276
57576.93050	16.0157	0.0410	-0.0893
57584.76134	16.1852	0.0308	-0.0615
57664.69172	16.1616	0.0256	0.0079
577B150278400 000.2271	RV	0.0761	$\sigma_{\text{RV}} - 0.075 \sigma_{\text{Bisector}}$
(UTC)	(km s ⁻¹)	(km s ⁻¹)	(km s ⁻¹)
Bisector errors are twice RV errors			
WASP-145:			
56811.88123	3.5320	0.0120	0.0275
56890.59823	3.1457	0.0173	0.0372
56903.76315	3.4954	0.0218	0.0133
56916.59725	3.4016	0.0184	0.0666
56927.67549	3.1723	0.0117	0.0048
56928.65445	3.5252	0.0117	0.0555
56942.63948	3.4927	0.0127	0.0234
56950.50317	3.2476	0.0128	0.0179
56956.50488	3.3369	0.0182	0.0057
56996.55409	3.1886	0.0164	-0.057
57140.91392	3.5285	0.0176	0.0123
57226.68125	3.1481	0.0368	0.0345
57295.70398	3.1732	0.0164	0.0375
57325.62279	3.2030	0.0242	0.0155
57493.89365	3.1607	0.0118	-0.042
57569.71114	3.2203	0.0146	0.0364
57584.85526	3.5170	0.0134	0.0052
57600.73014	3.5075	0.0253	-0.064
57629.57199	3.3861	0.0183	-0.028
WASP-158:			
56876.83406	24.4864	0.0402	-0.0026
57006.53670	23.9180	0.0557	0.1307
57007.59318	24.3047	0.0550	-0.1263
57008.60038	24.4297	0.0516	-0.1734
57010.57920	23.9154	0.0447	0.0440
57011.56783	24.4198	0.0492	-0.0777
57014.58938	24.1044	0.0440	0.0382
57203.89522	23.8789	0.0629	-0.0082
57205.82496	24.6116	0.0874	0.1649
57224.78600	24.2981	0.1224	0.1592
57255.72861	24.0305	0.0740	-0.0932
57302.75125	23.9124	0.1391	0.0988
57327.70752	23.9901	0.1039	0.0236
57370.56015	24.4935	0.0647	0.0285
57559.88888	24.3833	0.0641	0.2210
57587.77799	23.9875	0.0552	-0.0663
57598.84959	23.9258	0.0478	-0.0213
57613.72822	23.8843	0.0362	0.0952
57655.75797	24.4331	0.0518	0.0073
57692.71279	24.3341	0.0619	-0.1398

Bisector errors are twice RV errors

BJD – 2400 000 (UTC)	RV (km s ⁻¹)	σ_{RV} (km s ⁻¹)	Bisector (km s ⁻¹)
WASP-159:			
56979.72275	35.1927	0.0392	0.0045
57004.70593	35.1071	0.0370	-0.0080
57022.73682	35.1871	0.0320	0.0114
57033.65716	35.2266	0.0190	0.0563
57035.55510	35.0952	0.0291	-0.0921
57036.69928	35.2257	0.0272	0.0252
57061.57339	35.1507	0.0567	0.2588
57086.56873	35.1548	0.0242	0.0820
57089.53336	35.1237	0.0315	0.1049
57261.90726	35.0649	0.0432	0.0070
57286.75364	35.1981	0.0679	-0.1212
57331.79414	35.1973	0.0594	0.1496
57333.76731	35.1721	0.0343	0.0166
57338.78070	35.1030	0.0486	0.1369
57340.81000	35.1969	0.0391	0.0116
57367.67376	35.1806	0.0369	0.0566
57388.60652	35.1290	0.0325	0.0089
57390.66011	35.2368	0.0256	-0.0008
57398.60368	35.1855	0.0282	0.0600
57399.64861	35.1485	0.0356	-0.0326
57416.62863	35.1671	0.0354	-0.0714
57429.55929	35.2009	0.0189	0.0197
57689.81060	35.2180	0.0221	0.0669
57715.79980	35.1126	0.0517	0.2065
57726.65988	35.0920	0.0280	-0.0658
57751.67104	35.1994	0.0339	-0.0262
57770.62964	35.2220	0.0247	-0.0469
57806.59954	35.1281	0.0394	0.0558
57823.55477	35.1264	0.0294	-0.0393

Bisector errors are twice RV errors

BJD – 2400 000 (UTC)	RV (km s ⁻¹)	σ_{RV} (km s ⁻¹)	Bisector (km s ⁻¹)
WASP-162:			
56770.55906	16.5348	0.0125	-0.0527
57188.52985	16.8266	0.0307	-0.0684
57208.49314	17.2122	0.0586	-0.0831
57366.83385	16.6059	0.0227	-0.0727
57376.84521	16.5777	0.0256	-0.0523
57378.78780	16.5437	0.0281	-0.0457
57379.81346	16.6176	0.0162	-0.0212
57407.84558	16.5549	0.0275	-0.0920
57422.71696	16.8750	0.0139	-0.0533
57429.78462	17.1033	0.0171	-0.0017
57430.76149	17.5554	0.0176	-0.0021
57431.71535	17.1215	0.0166	-0.0121
57487.66160	17.1725	0.0186	-0.0134
57559.54335	16.5979	0.0167	-0.0601
57590.46580	16.5571	0.0178	-0.0355
57814.70374	17.0837	0.0167	-0.0047
57831.65846	16.5867	0.0146	-0.0366
57890.53621	16.7395	0.0251	-0.0334

Bisector errors are twice RV errors

BJD – 2400 000 (UTC)	RV (km s ⁻¹)	σ_{RV} (km s ⁻¹)	Bisector (km s ⁻¹)
WASP-168:			
56993.61587	50.4209	0.0207	-0.0119
57319.84988	50.5521	0.0650	-0.0670
57373.65989	50.4980	0.0201	-0.0666
57374.82620	50.4945	0.0206	-0.0182
57398.69788	50.4940	0.0197	-0.0573
57425.57334	50.4021	0.0158	-0.0500
57427.58986	50.5011	0.0103	-0.0211
57428.56442	50.4785	0.0138	-0.0039
57633.88933	50.4647	0.0279	-0.0214
57660.88579	50.4503	0.0208	0.0081
57661.74546	50.4431	0.0199	0.0232
57666.82069	50.4148	0.0417	-0.0413
57668.81582	50.5055	0.0151	-0.0186
57669.83349	50.4472	0.0140	0.0102
57671.87378	50.4937	0.0158	0.0062
57682.87937	50.4024	0.0148	0.0267
57694.80350	50.4516	0.0198	-0.0049
57699.80030	50.3893	0.0159	-0.0149
57715.69598	50.4021	0.0295	0.0145
57715.74476	50.4411	0.0259	-0.0132
57716.67587	50.3988	0.0221	-0.0235
57717.72294	50.4883	0.0180	-0.0209
57726.73304	50.5192	0.0168	-0.0345
57739.72958	50.4764	0.0152	-0.0684
57747.64158	50.5091	0.0153	-0.0041
57753.65099	50.4125	0.0159	-0.0474
57770.57567	50.4184	0.0170	0.0118
57800.63160	50.4685	0.0162	0.0179
57812.53164	50.4472	0.0311	0.0327
57824.61792	50.4071	0.0172	0.0106
57825.61993	50.4731	0.0155	-0.0168
57851.48939	50.5234	0.0207	0.0183
57855.54592	50.5380	0.0189	-0.0512

Bisector errors are twice RV errors

BJD – 2400 000 (UTC)	RV (km s ⁻¹)	σ_{RV} (km s ⁻¹)	Bisector (km s ⁻¹)
WASP-172:			
56032.82587	–20.2779	0.0376	–0.1099
56033.76992	–20.2324	0.0408	–0.2306
56067.68648	–20.2674	0.0335	–0.1889
56458.64357	–20.3749	0.0295	–0.0675
56480.58391	–20.3742	0.0486	–0.1607
56510.47908	–20.2984	0.0254	–0.1334
56684.80361	–20.2547	0.0293	–0.0681
56687.83916	–20.3135	0.0311	–0.1047
56688.81248	–20.3700	0.0266	–0.1500
56693.81486	–20.3164	0.0275	–0.0655
56696.83656	–20.2362	0.0282	–0.0877
56719.80357	–20.2472	0.0265	–0.1452
56726.64829	–20.1913	0.0306	–0.2492
56744.84931	–20.2370	0.0260	–0.1462
56746.65439	–20.1751	0.0274	–0.1812
56769.64903	–20.2818	0.0255	–0.2407
56771.73503	–20.3274	0.0289	–0.0003
56772.78389	–20.2638	0.0259	–0.1796
56810.66120	–20.2545	0.0329	–0.0537
56832.61861	–20.3054	0.0283	–0.2543
56837.57872	–20.3273	0.0318	–0.1202
56887.50487	–20.3078	0.0387	–0.1019
57110.75884	–20.3448	0.0373	–0.1166
57111.83467	–20.2970	0.0411	–0.2220
57112.82654	–20.2434	0.0510	–0.3006
57138.77562	–20.3384	0.0409	–0.2117
57192.49655	–20.3254	0.0481	–0.2102
57433.75786	–20.3380	0.0326	–0.1377
57485.79471	–20.2615	0.0305	–0.0924
57568.54383	–20.2230	0.0321	–0.2626
57599.53201	–20.2590	0.0301	–0.2653
57603.53378	–20.3060	0.0304	–0.1942
57617.49253	–20.2947	0.0404	–0.1868
57619.47611	–20.4079	0.0594	–0.0104
57901.63900	–20.2975	0.0558	–0.0185
57917.54541	–20.2397	0.0468	–0.1590
57918.46887	–20.2510	0.0551	–0.2097
57922.59777	–20.2494	0.0544	–0.3099

Bisector errors are twice RV errors

BJD – 2400 000 (UTC)	RV (km s ⁻¹)	σ_{RV} (km s ⁻¹)	Bisector (km s ⁻¹)
WASP-173:			
57278.67586	−7.3294	0.0220	−0.0142
57606.72588	−8.5150	0.0197	−0.0191
57613.69950	−8.4979	0.0143	0.0097
57625.65795	−7.4262	0.0178	−0.0341
57633.59834	−7.4199	0.0233	0.0263
57634.68392	−8.2375	0.0162	−0.0158
57637.62434	−7.8120	0.0174	−0.0004
57638.68631	−8.5166	0.0168	−0.0422
57639.77874	−8.1162	0.0141	−0.0480
57650.61128	−7.4410	0.0153	−0.0459
57654.61358	−7.2387	0.0231	−0.0011
57655.71970	−7.5596	0.0169	−0.0044
57659.63846	−8.2932	0.0164	0.0310
57689.62544	−7.9254	0.0139	−0.0421
57691.54377	−8.2317	0.0172	−0.0330
57716.56890	−8.0514	0.0242	0.0915
57718.59164	−7.5169	0.0225	−0.0307
57735.55690	−8.3275	0.0173	−0.0024

Bisector errors are twice RV errors

This paper has been typeset from a T_EX/L^AT_EX file prepared by the author.